Belyakov homoclinic bifurcation in three dimensions

Sara Bonacina, 1128701

2nd February 2026

Introduction

The aim of this essay is to analyze and understand the behavior of the Belyakov bifurcation point. This phenomenon represents a critical moment in three-dimensional systems dependent on parameters, where a homoclinic orbit Γ_0 undergoes a profound structural transformation.

The core of the analysis lies in the transition of the equilibrium point from a saddle (with real eigenvalues) to a saddle-focus (with complex conjugate eigenvalues). As we will demonstrate, this transition is not merely a change in local geometry but the origin of an extraordinary dynamical richness, including the birth of infinitely many periodic orbits and chaotic structures, with fundamental implications in biological models such as the FitzHugh-Nagumo system.

1 Belyakov Homoclinic bifurcation

Consider a generic $3D$ system depending on two parameters:

$$\dot{u} = F(u, \alpha), u \in \mathbb{R}^3, \alpha \in \mathbb{R}^2 \tag{1}$$

At $\alpha = 0$, the system has an equilibrium at the origin with a homoclinic orbit Γ_0. The defining characteristic of the Belyakov point is the configuration of its eigenvalues: at this critical state, the stable eigenvalues coincide ($\lambda_1 = \lambda_2 = \gamma_0 < 0$), marking the boundary between purely attractive behavior (real) and rotationally attractive behavior (complex). When the system moves away from this critical configuration, the symmetry breaking of the eigenvalues combined with the presence of the homoclinic orbit triggers a cascade of events described by the following theorem [4]:

Theorem 1. *Consider a smooth 3D system of ODE dependent upon 2 parameters, having at some parameter values a homoclinic orbit Γ_0 to the equilibrium $O = (0, 0, 0)$ with eigenvalues $\lambda_1 = \lambda_2 = \gamma_0 < 0$ and $\lambda_3 = \nu_0 > -\gamma_0$. Then the corresponding point in the parameter plane is the origin of 3 countable sets of bifurcation curves:*

1. $t_n^{(1)}$: *fold (or saddle-node) bifurcation curves of periodic orbits making one global passage near* Γ_0

2. $f_n^{(1)}$: *flip (or periodic doubling) bifurcation curves of periodic orbits making one global passage near* Γ_0

3. $h_n^{(2)}$: *bifurcation curves corresponding to the existence of saddle-focus homoclinic orbits making 2 global passage near* Γ_0

The curves t_n *and* f_n *accumulate exponentially fast at both sides on the saddle focus part of a bifurcation curve* $h^{(1)}$ *corresponding to the existence of a homoclinic orbit to the equilibrium making one global passage near* Γ_0 *while the curves* $h_n^{(2)}$ *do so at one side only. Geometrically, the curves* $h_n^{(2)}$ *are typically "interleaved" between the* t_n *and* f_n *curves. The orbits corresponding to the curves with bigger integer* $n \in \mathbb{N}$ *make more local turns near the equilibrium before the global passage*

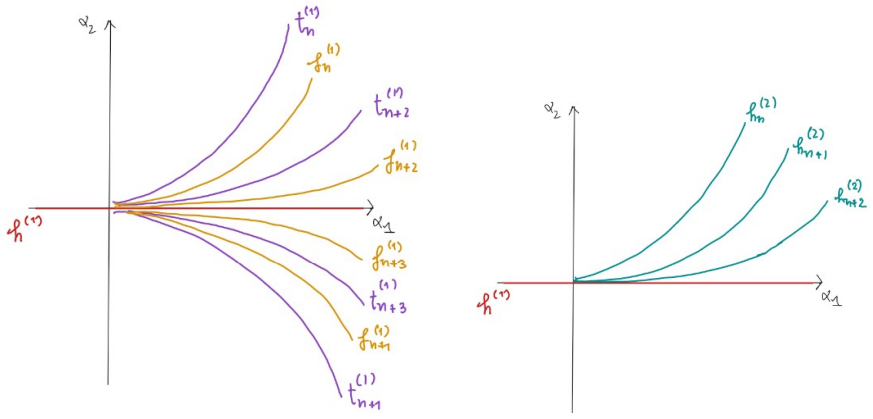

Figure 1: Bifurcation curves at the Belyakov point

Proof. The following proof of the Belyakov Theorem focuses on the construction and analysis of the Poincaré return map. In developing this argument, I will primarily follow the analytical framework presented in [4], while relying on the geometric and topological classification of homoclinic bifurcations provided by Kuznetsov in [6], [5].

First, making $O = (0, 0, 0)$ an equilibrium for every α, we transform the system smoothly near the critical parameter values $||\alpha|| = 0$. In particular, by applying a smooth change of coordinates near the equilibrium, the system can be written in a partial normal form where the vertical component is decoupled and linear. This transformation allows us to isolate the dynamics along one axis and focus on the unfolding of the double-real eigenvalue in the (x, y) plane. The system takes the form:

$$\begin{cases} \dot{x} = \gamma(\alpha)x + y + f_1(x,y,z,\alpha)x + f_2(x,y,z,\alpha)y \\ \dot{y} = -\alpha_1 x + \gamma(\alpha)y + g_1(x,y,z,\alpha)x + g_2(x,y,z,\alpha)y \\ \dot{z} = \lambda(\alpha)z \end{cases} \tag{2}$$

with $\alpha = (\alpha_1, \alpha_2), \gamma(0) = \gamma_0 < 0, \lambda(0) = \nu_0 > 0$ and $f_{1,2}, g_{1,2}$ smooth functions that vanish at the origin.
To ensure a standardized unfolding, we can set the specific normalization $f_1 \equiv g_2 = 2(\gamma(\alpha) - \gamma_0)$. This choice effectively absorbs unwanted variations of the real parts of the eigenvalues as α_1 varies, ensuring that α_1 exclusively controls the splitting of the eigenvalues without shifting their mean distance from the imaginary axis.

For $\alpha_1 = 0$ the equilibrium has a double real eigenvalue $\lambda_{1,2} = \gamma(0) = \gamma_0$ and $\lambda_3 = \nu(0) = \nu_0$.

If we set $\alpha_1 < 0$ then the eigenvalues of the equilibrium are real and simple while for $\alpha_1 > 0$ we have a simple pair of complex conjugate eigenvalues and a positive one.

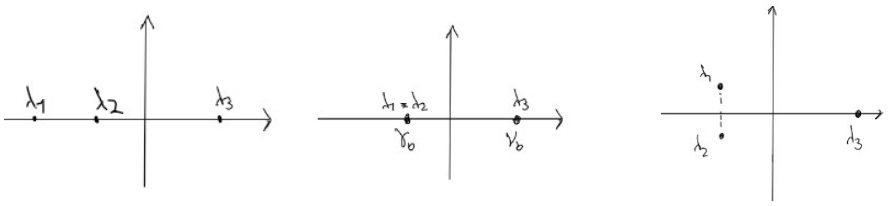

Figure 2: Eigenvalues for $\alpha_1 < 0$ (left, saddle), $\alpha_1 = 0$ (center, Belyakov bif. point) and for $\alpha_1 > 0$ (right, saddle-focus case)

Moreover, for sufficiently small $\|\alpha\|, O$ has an unstable manifold $\mathcal{W}^u(O)$ of 1 dimension, composed of two outgoing orbits Γ_1, Γ_2 corresponding to the z-axis ($x = 0,\ y = 0$) and a 2-dimensional stable manifold $\mathcal{W}^s(O)$ composed of all incoming orbits corresponding to the plane (x, y) ($z = 0$).

The orbit Γ_1 starts from the equilibrium O along the positive half of the unstable manifold, i.e, the positive half of the z-axis. The unstable manifold $\mathcal{W}^u(O)$ is locally characterized by the outgoing branch Γ_1. Under the hypothesis that there exists a homoclinic orbit Γ_0 at the critical parameter $\alpha = 0$, we can identify Γ_1 as the initial segment of this global trajectory. In this sense, the condition $\Gamma_1 = \Gamma_0$ signifies that the local unstable branch successfully returns to the origin, completing the loop. For $\alpha_2 \neq 0$, this identity breaks: Γ_1 still exists as a local departure from O, but it fails to reconnect with the stable manifold $\mathcal{W}^s(O)$, thus preventing the formation of the global orbit Γ_0. Therefore we can conclude that:

$$\forall\ |\alpha_1| \text{ small }, \alpha_2 = 0,\ \exists\ \Gamma_0 \text{ homoclinic orbit to O.}$$

Specifically, as illustrated in Figure 3, Γ_0 is a homoclinic orbit to the saddle equilibrium O for $\alpha_1 < 0$ and to the saddle-focus equilibrium O for $\alpha_1 > 0$.

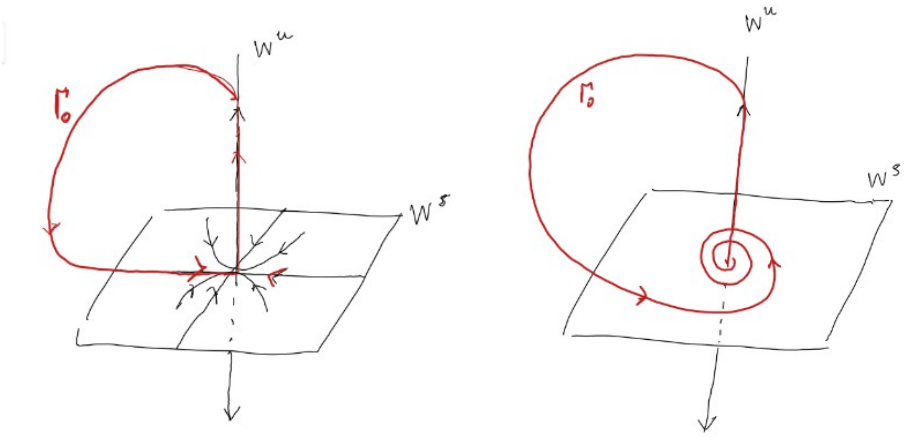

Figure 3: Stable and unstable manifold with homoclinic orbit Γ_0 in the saddle and saddle-focus cases respectively

Our aim is to analyze the bifurcation diagram of the system for small $\|\alpha\|$ in the half-plane $\alpha_1 > 0$, in the case $\nu_0 > -\gamma_0$, i.e. for a positive saddle quantity $\sigma_0 = \gamma_0 + \nu_0 > 0$.

In this regime the equilibrium is a saddle-focus in which expansion along the unstable direction dominates contraction in the stable directions. For the Belyakov bifurcation to unfold its full complexity, the primary homoclinic loop Γ_0 must possess a twisted geometry. Under this condition, the interaction between the local spiraling dynamics near the saddle-focus ($\alpha_1 > 0$) and the global return along the homoclinic loop produces an oscillatory Poincaré return map [5]. As a result, infinitely many bifurcation curves accumulate exponentially.

In contrast, when the saddle quantity is negative ($\sigma_0 < 0$), contraction toward the equilibrium is dominant. In this case, regardless of whether the homoclinic loop is twisted or non-twisted, the dynamics near the homoclinic orbit is significantly simpler: a unique stable limit cycle bifurcates from the primary homoclinic orbit for $\alpha_2 > 0$, and no accumulation of secondary bifurcation curves occurs.

To analyze the behaviour of the system near the bifurcation, we can reduce the analysis to a Poincarè map near the homoclinic orbit Γ_0.

We define two local cross-sections as follows. Let Σ^- be a plane parallel to the (x, y)-plane at $z = h > 0$, and let Σ^+ be a transverse section to the stable manifold, for instance $\Sigma^+ = \{(x, y, z) : \sqrt{x^2 + y^2} = \delta\}$, with $\delta > 0$ sufficiently small. With this choice, Σ^+ is an entry section and Σ^- is an exit section for the flow near the equilibrium.

The Poincaré map $P : \Sigma^+ \to \Sigma^+$, as we can see in Figure 4, is defined as the composition of two maps

$$P = Q \circ \Delta$$

where $\Delta : \Sigma^+ \to \Sigma^-$ is the singular local map near the equilibrium, and $Q : \Sigma^- \to \Sigma^+$ is the regular global map along the homoclinic orbit.

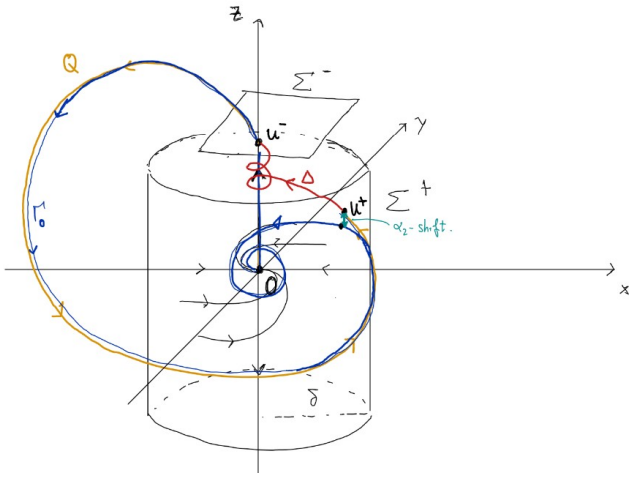

Figure 4: Poincarè Map $P = Q \circ \Delta$, homoclinic curve Γ_0

Local map $\Delta : \Sigma^+ \to \Sigma^-$

Near the equilibrium, we consider the linearized system with eigenvalues $\lambda_{1,2} = \gamma(\alpha) \pm i\omega(\alpha)$ $(\gamma(\alpha) < 0)$ and $\lambda_3 = \nu(\alpha) > 0$.
We also define $\gamma(0) = \gamma, \nu(0) = \nu$.

Introducing polar coordinates (ρ, θ) in the stable plane, points on Σ^+ are described by (ρ, θ, z_0), where $\rho = \delta$ is fixed and z_0 measures the distance from the stable manifold.

We can rewrite the system in polar coordinates:

$$\begin{cases} \dot{\rho} = \gamma\rho \\ \dot{\theta} = \omega \\ \dot{z} = \nu z \end{cases}$$

The time τ required for a trajectory starting at $u_0 = (x_0, y_0, z_0)$ to reach the exit section Σ^- is determined by the unstable component,

$$z(\tau) = z_0 e^{\nu\tau} = h,$$

which yields

$$\tau(z_0) = \frac{1}{\nu} \ln \frac{h}{z_0}.$$

As $z_0 \to 0^+$, the flight time satisfies $\tau(z_0) \to +\infty$.

During the time interval $[0, \tau]$, the motion in the stable directions is given by

$$\rho(t) = \delta e^{\gamma t}, \qquad \theta(t) = \theta_0 + \omega t.$$

Evaluating these expressions at $t = \tau(z_0)$, we obtain

$$\rho(\tau) = C\, z_0^{\beta}, \qquad \theta(\tau) = \theta_0 - \Omega \ln z_0 + \text{const},$$

where

$$\beta = -\frac{\gamma}{\nu} > 0, \qquad \Omega = \frac{\omega}{\nu},$$

and $C > 0$ is a constant.

Projecting the flow onto the exit section Σ^-, the local map $\Delta : \Sigma^+ \to \Sigma^-$ therefore has the asymptotic form

$$\Delta(z_0, \theta_0) = z_0^{\beta} \begin{pmatrix} \cos(\theta_0 - \Omega \ln z_0 + \phi) \\ \sin(\theta_0 - \Omega \ln z_0 + \phi) \end{pmatrix} + o(z_0^{\beta}),$$

where ϕ is a constant depending on the choice of the sections.

The logarithmic dependence on z_0 reflects the spiraling of trajectories near the saddle-focus equilibrium and is responsible for the singular nature of the local map.

Global map $Q : \Sigma^- \to \Sigma^+$

The global map Q describes the flow along the regular part of the orbit Γ_0 (far from the equilibrium). Using a Taylor expansion near the re-entry point, we approximate Q as an affine transformation. In particular, up to higher–order terms, the global return induces a shift in the distance from the stable manifold, which can be written as

$$z \mapsto \alpha_2 + az,$$

where α_2 is the homoclinic splitting parameter and $a \neq 0$ is a constant.

When $\alpha_2 = 0$, the unstable manifold returns exactly to the stable manifold, forming the homoclinic orbit.

Composing the local map $\Delta : \Sigma^+ \to \Sigma^-$ with Q, we obtain the Poincaré map:

$$P = Q \circ \Delta : \Sigma^+ \to \Sigma^+$$

Although the Poincaré map $P = Q \circ \Delta$ is defined on the 2-dimensional section Σ^+, its essential dynamics near the homoclinic orbit can be captured by a 1-dimensional reduction. Indeed, the angular variable θ enters the local map only through the oscillatory term $\cos(\theta_0 - \Omega \ln z_0 + \phi)$ and does not affect the distance to the stable manifold at leading order.

Moreover, the strong contraction in the stable directions implies that nearby trajectories rapidly align along the most expanding direction transverse to the stable manifold.

As a consequence, the existence and bifurcation of periodic and homoclinic orbits are determined by the evolution of the scalar variable z_0, which measures the distance from the stable manifold on the entry section Σ^+.

Fixing a reference phase and neglecting higher-order angular corrections, the Poincaré map can therefore be asymptotically reduced to a 1-dimensional map of the form:

$$P(z_0) = \alpha_2 + A\, z_0^{\beta} \cos(\Omega \ln z_0 + \phi) + \dots,$$

where

$$\beta = -\frac{\gamma}{\nu} > 0, \qquad \Omega = \frac{\omega}{\nu},$$

and A and ϕ are constants depending on the linearization and on the choice of the sections. We can now identify the conditions for the three types of bifurcations mentioned in the theorem: we know that fixed points of the map P correspond to periodic orbits of the flow. The following bifurcations occur when these fixed points are degenerate:

1. **Fold (Saddle-Node) Bifurcation (t_n):** $P(z_0) = z_0$ and $P'(z_0) = 1$.
2. **Period-Doubling (Flip) Bifurcation (f_n):** $P(z_0) = z_0$, $P'(z_0) = -1$.
3. **Secondary Homoclinic Bifurcation (h_n):** $P(z_0) = 0$ (for $z_0 \neq 0$).

The oscillatory term $\cos(\Omega \ln z_0 + \phi)$ implies that as $z_0 \to 0^+$, the map and its derivative

$$P'(z_0) = A z_0^{\beta-1} \big[\beta \cos(\Omega \ln z_0 + \phi) - \Omega \sin(\Omega \ln z_0 + \phi)\big] + \dots$$

oscillate infinitely many times. If the saddle quantity is positive, $\sigma = \gamma + \nu > 0$ (so that $\beta < 1$), the derivative behaves as

$$|P'(z_0)| \sim z_0^{\beta-1} \to +\infty \quad \text{as } z_0 \to 0^+,$$

ensuring that the oscillations of the map are strong enough to satisfy the bifurcation conditions infinitely often for sufficiently small α_2.

The integer $n \in \mathbb{N}$ represents the number of full rotations a trajectory performs near the saddle-focus equilibrium before leaving along the unstable manifold. As $n \to \infty$, the orbits start closer to the stable manifold ($z_0 \to 0$) and spend more time near the equilibrium, which corresponds to an increasing number of local turns in the neighborhood of O before the global excursion begins.

The difference in the accumulation behavior of these curves can be understood by examining the geometry of the Poincaré map. Since we are considering the case with a positive saddle quantity ($\sigma > 0$, implying $\beta < 1$), the derivative of the map $P'(z_0) \sim z_0^{\beta-1}$ diverges as $z_0 \to 0^+$. This implies that the oscillations of $P(z_0)$ become increasingly "vertical" and their amplitude z_0^{β} dominates the linear term z_0 near the origin. For the periodic orbit bifurcations (t_n and f_n), the fixed point condition $P(z_0) = z_0$ (with $P'(z_0) = \pm 1$) can be satisfied for both $\alpha_2 > 0$ and $\alpha_2 < 0$. Even when the splitting parameter α_2 is negative, as we can observe in Figure 5, the expanding oscillations of the map are sufficiently large to "reach back" and intersect the diagonal $y = z_0$, leading to the bilateral accumulation of t_n and f_n on the primary homoclinic line $\alpha_2 = 0$.

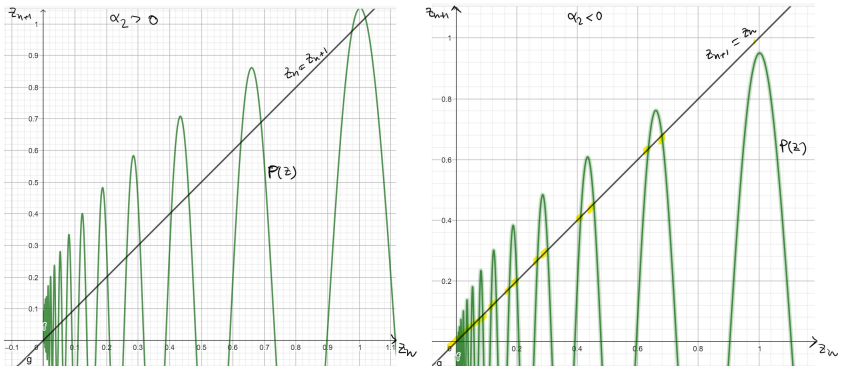

Figure 5: $P(z)$ intersect $z_n = z_n + 1$ for $\alpha_2 > 0$ and $\alpha_2 < 0$

Conversely, the secondary homoclinic orbits $h_n^{(2)}$ require the unstable manifold $\mathcal{W}^u(O)$ to return to the origin after exactly two global passages, as we can see in figure 6.

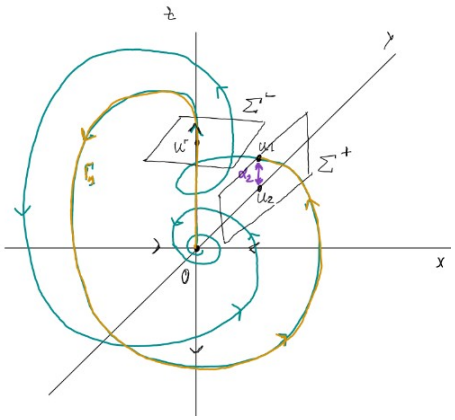

Figure 6: Secondary homoclinic bifurcations (for simplicity here Σ^+ is a plane and not a cylinder)

After the first passage, the unstable manifold (which corresponds to $z_0 = 0$) returns to the section Σ^+ at the point $u_1 = (x_1, y_1, z_1)$ with $z_1 = P(0) = \alpha_2$. For a second circuit to occur, this point must lie on the "active" side of the stable manifold ($z_1 > 0$) to be reinjected into the neighborhood of the equilibrium. If $\alpha_2 < 0$, the manifold is shifted away from the local spiraling region, and no secondary homoclinic orbit can be formed. Therefore, the curves $h_n^{(2)}$ accumulate on the line $h^{(1)}$ from the side $\alpha_2 > 0$ only.

This concludes the argument for the existence of the bifurcation structure at the Belyakov point.

□

2 Implications in a mathematical model: Existence of complicated travelling waves in the FitzHugh-Nagumo model

This section is based on the works of Keener and Sneyd [3] and Kuznetsov [6]. To understand the implications of the Belyakov bifurcation, we study the FitzHugh-Nagumo (FHN) model, a cornerstone of electrophysiology. The FHN model is a simplified version of the Hodgkin-Huxley model (1952), which described nerve impulse propagation along a squid giant axon using four nonlinear ODEs based on ionic currents (Na^+, K^+). Around ten years later, FitzHugh and Nagumo extracted the essential "fast-slow" dynamics into a 2-variable PDE system:

$$\begin{cases} \dot{u} = \frac{\partial u}{\partial t} = \frac{\partial^2 u}{\partial x^2} - f_a(u) - v \\ \dot{v} = \frac{\partial v}{\partial t} = bu \end{cases} \tag{3}$$

Here $u(x,t)$ is the "fast" excitation variable, represents the membrane potential, while $v(x,t)$ is the "slow" recovery variable. It acts as a negative feedback bringing the system back to rest. In the equation for u there is a cubic reaction term:

$$f_a(u) = u(u-a)(u-1)$$

that depends on a parameter $0 < a < 1$. It facilitates the excitability. We also know that $b > 0, u(x,t) : x \in (-\infty, \infty), t > 0$.

We are looking for travelling wave solutions of the form $u(x,t) = U(\xi)$, $v(x,t) = V(\xi)$, where $\xi = x + ct$ and c is the propagation speed. In particular, with this setting, we have that if $c > 0$ then the wave is moving from right to the left and in the opposite direction if $c < 0$. Recall that we talk about travelling wave or front if

$$\lim_{t \to +\infty} u(x,t) = k \neq h = \lim_{t \to -\infty} u(x,t)$$

and about travelling pulse if $h = k$

Figure 7: Travelling wave and Travelling pulse

Since $U(\xi) = U(x + ct)$, we have $u_t = cU_\xi, u_x = U_\xi, v_t = cV_\xi$, hence,

substituting into the PDE yields a 3D system of ODEs:

$$\begin{cases} \dot{U} = U_\xi = W \\ \dot{W} = cU_\xi + f_a(U) + V = cW + f_a(U) + V \\ \dot{V} = V_\xi = \frac{b}{c}U \end{cases} \tag{4}$$

Any bounded orbit of the wave system corresponds to a travelling wave solution of the FitzHugh-Nagumo system at parameter (a, b) propagating with velocity c.

We fix $c > 0$. We can observe that the system has a unique equilibrium in the origin: $E_0 = (0, 0, 0)$. Thus, the system at the origin is at the steady state. An homoclinic orbit to the equilibrium E_0 represents a travelling pulse (an action potential that starts and ends at the resting state).

The Jacobian matrix is given by

$$J(U, W, V) = \begin{pmatrix} 0 & 1 & 0 \\ f_a'(U) & c & 1 \\ \frac{b}{c} & 0 & 0 \end{pmatrix}$$

where $f_a'(u) = 3u^2 - 2u(a + 1) + a$. The Jacobian evaluated at the equilibrium point is

$$\begin{pmatrix} 0 & 1 & 0 \\ a & c & 1 \\ \frac{b}{c} & 0 & 0 \end{pmatrix}$$

Therefpre, the characteristic polynomial is

$$P(\lambda) = \lambda^3 - c\lambda^2 - a\lambda - \frac{b}{c} = 0$$

By Descartes' Rule of Signs, the sequence of coefficients for $P(\lambda)$ is $(+, -, -, -)$. Since there is exactly one sign change, the system possesses exactly one real positive eigenvalue, $\lambda_1 > 0$. Furthermore, evaluating the polynomial at $\lambda = c$ gives:

$$P(c) = c^3 - c(c^2) - ac - \frac{b}{c} = -\left(ac + \frac{b}{c}\right) < 0$$

Since $P(c) < 0$ and $P(\lambda) \to +\infty$ as $\lambda \to \infty$, it follows that the positive eigenvalue must satisfy $\lambda_1 > c$. The relationship between the eigenvalues is governed by Viète's formulas:

- $\lambda_1 + \lambda_2 + \lambda_3 = \mathrm{Tr}(J) = c$
- $\lambda_1\lambda_2\lambda_3 = \det(J) = \frac{b}{c}$

Since $\lambda_1 > c$, the sum of the remaining roots must be negative: $\lambda_2 + \lambda_3 = c - \lambda_1 < 0$. This implies that $\lambda_{2,3}$ are either real and negative or complex conjugates with a negative real part ($\mathrm{Re}(\lambda_{2,3}) < 0$). In either case, E_0 is a saddle or saddle-focus equilibrium.

The Belyakov bifurcation occurs when the stable eigenvalues $\lambda_{2,3}$ change from real to complex. This transition happens on the surface in the parameter space (a, b, c) where the discriminant Δ of $P(\lambda)$ vanishes. On one side of this boundary ($\Delta > 0$), E_0 is a standard saddle; on the other ($\Delta < 0$), E_0 is a saddle-focus.

The transition from real to complex roots is governed by the discriminant Δ. Recall that for a general cubic equation in the form $\lambda^3 + B\lambda^2 + C\lambda + D = 0$, the discriminant Δ is defined as:

$$\Delta = 18BCD - 4B^3D + B^2C^2 - 4C^3 - 27D^2$$

By matching the coefficients of our characteristic equation, we set:

$$B = -c, C = -a, D = -\frac{b}{c}$$

Substituting these into the general formula yields:

$$\Delta = -18ab - 4bc^2 + a^2c^2 + 4a^3 - \frac{27b^2}{c^2}$$

Defining the Discriminant Function $\mathcal{D}$ to eliminate the denominator and focus on the sign of the discriminant, we define $\mathcal{D}(a, b, c) = -c^2\Delta$. Multiplying each term by $-c^2$ results in:

$$\mathcal{D} = 18abc^2 + 4bc^4 - a^2c^4 - 4a^3c^2 + 27b^2$$

Grouping the expression by powers of c, we arrive at the final analytical condition:

$$\mathcal{D} = c^4(4b - a^2) + 2ac^2(9b - 2a^2) + 27b^2$$

Fixing the parameter b, we can plot the discriminant curve $\mathcal{D}_b$ and the primary pulse curve $P_b^{(1)}$ on the (a, c) plane. This allows us to visualize the transition from the saddle to the saddle-focus regime at their intersection point:

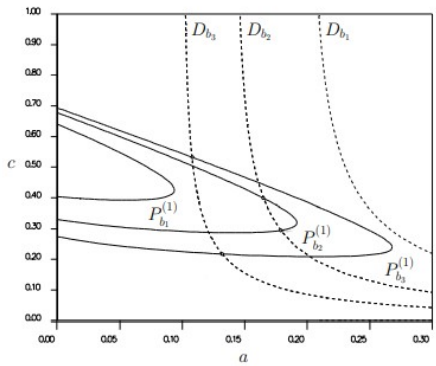

Figure 8: Bifurcation curves of the wave system for $b_1 = 0.01, b_2 = 0.005, b_3 = 0.0025$ [6]

In this diagram, $P_b^{(1)}$ (Primary Pulse) represents the global bifurcation curve where the system admits a solitary traveling wave solution. The intersection of $P_b^{(1)}$ with the algebraic locus $\mathcal{D}_b = 0$ identifies the Belyakov point, which acts as the threshold for structural changes in the wave's profile. The sign of $\mathcal{D}$ along the $P_b^{(1)}$ curve determines the geometry of the flow near the origin: $\mathcal{D} > 0 \implies \Delta < 0$: The system possesses one real eigenvalue and two complex conjugate eigenvalues. This identifies the origin as a saddle-focus, the required configuration for the existence of an oscillatory homoclinic pulse (a wave with an oscillating tail). $\mathcal{D} < 0 \implies \Delta > 0$: All eigenvalues are real, corresponding to a pure saddle and monotonic wavefront dynamics (a pulse that returns to rest without oscillations). This transition directly dictates the physical shape of the homoclinic orbits in the two cases:

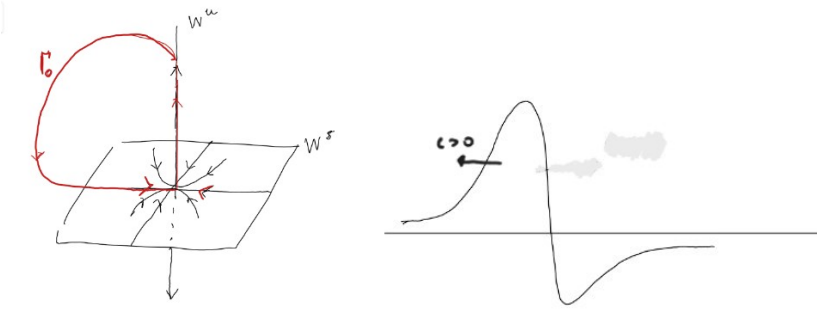

Figure 9: Travelling wave corresponding to homoclinic orbit to a saddle

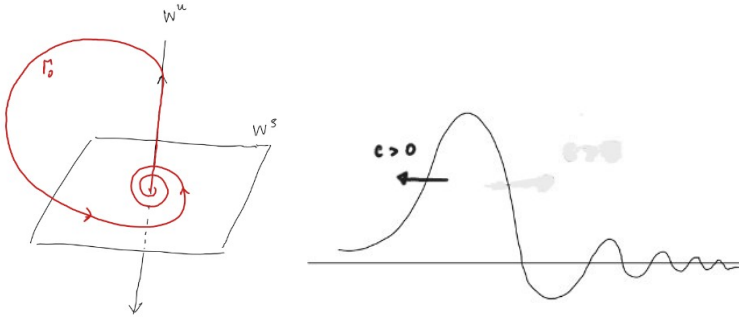

Figure 10: Travelling wave corresponding to homoclinic orbit to a saddle-focus

The maximum of the travelling wave corresponds to the peak of the action potential in the Fitz-Hugh Nagumo system, while the subsequent minimum corresponds to the hyperpolarization phase, which characterizes the neuron's refractory period. When the parameters satisfy the saddle-focus condition ($\mathcal{D} > 0$), the wave does not return to the resting state monotonically. Instead, it

exhibits an oscillating tail. This tail consists of a sequence of damped oscillations where the membrane potential rings around the equilibrium point. This behavior is the physical manifestation of the complex eigenvalues of the Jacobian matrix, which force the homoclinic orbit to spiral into the stable manifold of the origin as $\xi \to \infty$.

Applying the Belyakov theorem to this model leads to profound implications:

- For $\Delta > 0$ we are in the saddle case: the homoclinic orbit Γ_0 is unique and simple, corresponding to a single isolated impulse with a monotonic tail.
- For $\Delta = 0$ we are in the point of Belyakov bifurcation.
- For $\Delta < 0$ we are in the saddle-focus case. If the saddle quantity $\sigma = \mathrm{Re}(\lambda_{2,3}) + \lambda_1 > 0$, the theorem guarantees a rich bifurcation structure emerging from the Belyakov point:

    1. **Periodic Wave Trains (Limit Cycles):** The theorem predicts countable sets of bifurcation curves ($t_n^{(1)}$ and $f_n^{(1)}$). These curves represent fold and period-doubling bifurcations of periodic orbits. Physically, these orbits correspond to stable **periodic wave trains**, a continuous, self-sustaining sequence of neural impulses firing at a constant frequency.

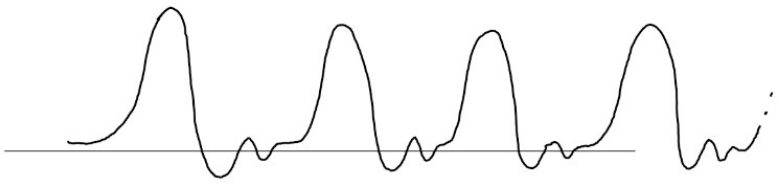

Figure 11: Periodic Wave Trains

    2. **Multi-pulses (Secondary Homoclinics):** The theorem further identifies curves ($h_n^{(N)}$) corresponding to the existence of N-homoclinic orbits. These are complex trajectories that do not return to the equilibrium point after a single excursion; instead, they perform N global passages in the neighborhood of the primary orbit Γ_0 before eventually closing at the origin. In the context of the travelling wave, each passage near the equilibrium corresponds to a distinct firing event. Thus, an N-homoclinic orbit manifests as an N-peak pulse (or multi-pulse).
    These are localized solutions where N individual impulses are locked together, travelling at the same speed c as a single unit. This locking is made possible by the oscillatory (spiraling) nature of the saddle-focus stable manifold, which allows the tail of one pulse to provide

the "kick" necessary to trigger the next one in a fixed spatial configuration.

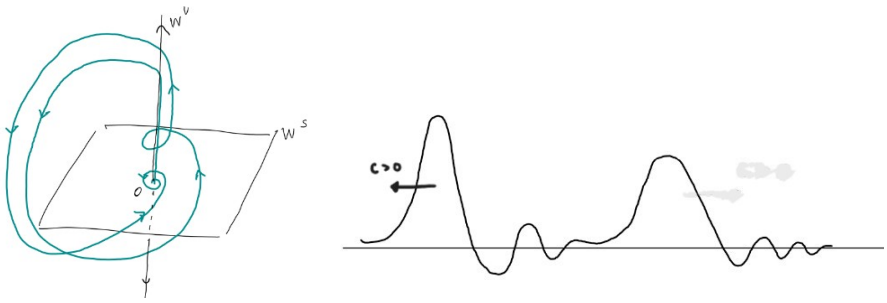

Figure 12: Double travelling impulse corresponding to secondary homoclinic orbits

In the FHN model, for $c > 0$, the condition $\sigma > 0$ is generally satisfied. Indeed, looking at the Jacobian matrix at the equilibrium, we have $Tr(J) = c > 0$ and we know that the Trace corresponds to the sum of the eigenvalues hence $\lambda_1 + 2\alpha = c$ where α is the real part of $\lambda_{2,3}$. From this relation, we can find $\alpha = \frac{c-\lambda_1}{2}$. Therefore $\sigma = \lambda_1 + Re(\lambda_{2,3}) = \lambda_1 + \alpha = \lambda_1 + \frac{c-\lambda_1}{2} = \frac{\lambda_1+c}{2} > 0$. Thus, the Belyakov bifurcation explains the transition from simple nerve impulses to complex, multi-peak patterns and periodic firing observed in excitable media.

Conclusions

The analysis of the Belyakov bifurcation reveals how the transition from a saddle to a saddle-focus acts as an organizing center for dynamical complexity. Through the construction of the Poincaré map, we have demonstrated that the positive saddle quantity condition ($\sigma > 0$) allows logarithmic oscillations to dominate the local dynamics, leading to the formation of infinitely many bifurcation branches. The application to the FitzHugh-Nagumo model illustrates the phenomenological value of this theory providing a rigorous mathematical explanation for the transition from simple nerve impulses to complex firing patterns, such as periodic wave trains and multi-peak pulses.

However, it is important to acknowledge the assumptions underlying this framework. The reduction of electrophysiological phenomena to a three-dimensional ODE system via the travelling wave coordinate, presumes a fast-slow separation that may overlook high-dimensional effects present in the original Hodgkin-Huxley equations. Furthermore, our analysis assumes a perfectly twisted homoclinic orbit; while this topology is a generic requirement for the full Belyakov complexity, its experimental verification in biological tissue remains an open challenge.

From a practical perspective, the exponential accumulation of the bifurcation curves t_n, f_n, and $h_n^{(2)}$ toward the primary homoclinic $h^{(1)}$, explains why multi-pulses and complex wave trains are notoriously difficult to detect, both in numerical simulations and experimental setups.

Because these curves converge at an exponential rate, the parametric regions where stable multi-pulses exist become infinitesimally thin as they approach the primary wave curve. Without the theoretical framework provided by Belyakov's theorem, finding these solutions by chance is nearly impossible; they are hidden within extremely narrow windows of the parameter space. Furthermore, the increasing number of local turns (represented by higher n) makes these waves highly sensitive to noise and numerical precision.

Looking forward, the insights gained here open several avenues for research. A natural extension would be the study of Belyakov-type dynamics in higher-dimensional media, such as spiral waves in cardiac tissue, where spatial curvature interacts with the local saddle-focus geometry.

Ultimately, studying this bifurcation not only enriches the theory of dynamical systems but also offers an essential framework for interpreting chaos and self-organization in excitable media, confirming that the geometry of homoclinic orbits is a key to understanding complex biological processes.

References

[1] Gianni Arioli and Hans Koch. "Existence and stability of traveling pulse solutions of the FitzHugh–Nagumo equation". In: *Nonlinear Analysis: Theory, Methods & Applications* 113 (2015), pp. 51–70.

[2] L. A. Belyakov. "Bifurcation of systems with homoclinic curve of a saddle-focus with saddle quantity zero". In: *Mathematical Notes of the Academy of Sciences of the USSR* 36 (1984), pp. 838–843.

[3] James Keener and James Sneyd. *Mathematical Physiology I: Cellular Physiology*. 2nd ed. Vol. 8. Interdisciplinary Applied Mathematics. New York: Springer, 2010.

[4] Yu. A. Kuznetsov, O. De Feo, and S. Rinaldi. "Belyakov Homoclinic Bifurcations in a Tritrophic Food Chain Model". In: *SIAM Journal on Applied Mathematics* 62.2 (2001), pp. 462–487.

[5] Yu.A. Kuznetsov. *Applied Nonlinear Dynamics*. Utrecht University University of Twente, 2023.

[6] Yuri A. Kuznetsov. *Elements of Applied Bifurcation Theory*. 2nd ed. Vol. 112. Applied Mathematical Sciences. New York: Springer, 1998.